Prevalent conformations and subunit exchange in the biologically active apoptin protein multimer

Leliveld, S.R.; Noteborn, M.H.M.; Abrahams, J.P.

Eur. J. Biochem. **270**, 3619–3627 (2003) © FEBS 2003 doi:10.1046/j.1432-1033.2003.03750.x

Prevalent conformations and subunit exchange in the biologically active apoptin protein multimer

Sirik R. Leliveld[1]*, Mathieu H. M. Noteborn[2,3] and Jan Pieter Abrahams[1]

[1]*Department of Chemistry, Leiden University, The Netherlands;* [2]*Leadd BV, Leiden, The Netherlands;* [3]*Department of Molecular Cell Biology, Leiden University Medical Center, Leiden, The Netherlands*

Recombinant, bacterially expressed apoptin protein induces apoptosis in human tumour cell lines but not in normal cells, mimicking the behaviour of ectopically expressed apoptin. Recombinant apoptin is isolated exclusively as a highly stable multimeric complex of 30–40 monomers, with little, if any, α-helical and β-sheet structure. Despite its apparent disorder, multimeric apoptin is biologically active. Here, we present evidence that most of the apoptin moieties within the complex may well share a similar conformation. Furthermore, the multimer has extensive and uniform hydrophobic patches and conformationally stable domains. Only a small fraction of apoptin subunits can exchange between multimers under physiologically relevant conditions. These results prompt a model in which the apoptin multimer has a highly stable core of nonexchangeable subunits to which exchangeable subunits are attached through hydrophobic interactions. In combination with previous findings, our results lead us to propose that the stable core of apoptin is the biologically relevant structure.

Keywords: apoptin; conformer; multimer; self-exchange; tumour-specific apoptosis.

In a recent paper, we reported that the viral protein apoptin is active as a tumour-specific apoptosis-inducing agent, even when expressed recombinantly in *Escherichia coli* and microinjected into human cells [1]. Furthermore, we demonstrated that the biologically active recombinant apoptin protein associates into highly stable complexes of 30–40 monomers that do not need to dissociate to induce apoptosis [2]. We showed that the hydrophobic N-terminal domain of apoptin, residues 1–69, is responsible for multimer formation, and by CD spectroscopy we established that the apoptin moieties are largely devoid of both α-helical and β-sheet structure [2]. These observations prompted the question whether the apoptin subunits adopt a well-defined, uniform conformation within its multimeric complex, or whether the observed multimers are the manifestation of a micellar phase of the apoptin protein in a more random conformation reflecting a (partially) unfolded state.

Here, we assessed the dynamics and level of conformational uniformity in the apoptin protein multimer by probing its surface with fluorescent reporter molecules. We used two different protein constructs: an N-terminal maltose-binding protein (MBP)–apoptin fusion protein, which could be expressed as soluble multimers in *E. coli*, and a hexahistidine-tagged apoptin, which could be refolded *in vitro* into soluble multimers. Both constructs are biologically active and induce tumour-specific apoptosis upon microinjection into cells [1,2]. First, we found that both constructs had comparable 4,4′-dianilino-1,1′-binaphthyl-5,5′-disulfonic acid (bis-ANS)-binding characteristics, suggesting that both constructs form a similar multimer despite the presence in MBP–apoptin of a large, highly soluble protein tethered to the N-terminus of apoptin. Secondly, the dye-binding behaviour of MBP–apoptin suggested that certain conformers were particularly abundant in the multimeric complex. This finding was in accordance with the apparent homogeneity of the conformation of the C-terminal domain of apoptin (residues 70–121), as inferred from the properties of fluorescent labels attached to the single exposed Cys residue of apoptin (Cys90). Using an assay based on fluorescence resonance energy transfer (FRET), we demonstrated that a minority of apoptin subunits are exchanged between the multimers under physiologically relevant conditions, indicating that not all apoptin molecules within the complex are equivalent in space and/or time. When performed in cell lysates, the rate of the exchange reaction was decreased, suggesting that cellular factors bind to the exchangeable fraction of apoptin molecules. Our data are consistent with a model of a highly stable multimer with an ordered core of nonexchanging apoptin molecules which are present in a largely uniform conformation devoid of regular secondary structure. Furthermore, the model has to assume that this core has substantial hydrophobic patches on its surface, to which exchangeable apoptin molecules stick. These data will be essential in elucidating the tumour-specific killing

Correspondence to J. P. Abrahams, PO Box 9502, 2300 RA, Leiden, The Netherlands.
Fax: + 31 (0)71 527 4357, Tel.: + 31 (0)71 527 4213,
E-mail: abrahams@fwncism1.leidenuniv.nl

Abbreviations: bis-ANS, 4,4′-dianilino-1,1′-binaphthyl-5,5′-disulfonic acid; Nbs_2, 5,5′-dithiobis(2-nitrobenzoic acid); FM, fluorescein-5-maleimide; FRET, fluorescence resonance energy transfer; NBD, *N*,*N*′-dimethyl-*N*-(iodoacetyl)-*N*′-(7-nitrobenz-2-oxa-1,3-diazol-4-yl) ethylenediamine; IA, 5-({[(2-iodoacetyl)amino]ethyl}amino)naphthalene-1-sulfonic acid; MBP, maltose-binding protein; PM, pyrene-*N*-maleimide.

Proteins: chicken anaemia virus VP3 (Cux1)/Apoptin®, Q99152.

**Present address*: Institute for Neuropathology, Heinrich-Heine University Medical School, Düsseldorf, Germany.

(Received 30 March 2003, revised 20 June 2003, accepted 14 July 2003)

mechanism of apoptin protein as they provide a means of identifying the essential conformations in the apoptin multimer.

Materials and methods

Cloning of MBP–apoptin triple Cys→Ser mutant

Part of the 5′ region of the apoptin ORF (nucleotides 1–155) was amplified by PCR using an internal 3′ primer that contained the C47S and C49S point mutations (TGC → TCC). This PCR fragment was digested with *Tse*I and then ligated with the flanking apoptin ORF fragment (nucleotides 156–366) that had been isolated after *Tse*I digestion of the full-length wild-type apoptin ORF (nucleotides 1–366). The reconstituted apoptin ORF was cloned at *Nde*I and *Not*I into pET-22b (Novagen), yielding pET-22bVp3(C47/49S). Using this clone, the procedure was repeated with an internal primer containing a C30S mutation. During this step, the PCR fragment and apoptin ORF were digested with *Bsp*EII. The apoptin ORF containing all three point mutations was cloned in pMalTB at *Bam*HI and *Sal*I. The clone (pMalTB-Vp3(C30/47/49S) was confirmed by sequencing.

Free Cys determination

For determination of Cys reactivity [3], fresh stock solutions of 5,5′-dithiobis(2-nitrobenzoic acid) (Nbs_2, 10 mM) (Sigma) and CysHCl (100 mM) (Fluka) were prepared in assay buffer: 0.1 M BisTris/HCl, pH 7.0, 1 mM EDTA. CysHCl and freshly prepared MBP–apoptin and H_6-MBP were diluted to 15 μM equivalent monomer concentration ([monomer]). After adding Nbs_2 to 250 μM, samples (including one blank) were incubated at 25 °C. A_{412} was measured after 2 and 20 min and after 1 h. H_6-MBP displayed no significant reactivity with Nbs_2.

Fluorescent labelling

Fluorescent labels. (1) *N*,*N*′-dimethyl-*N*-(iodoacetyl)-*N*′-(7-nitrobenz-2-oxa-1,3-diazol-4-yl)ethylenediamine (NBD), dissolved in methanol; (2) 5-({[(2-iodoacetyl)amino] ethyl}amino)naphthalene-1-sulfonic acid (IA), dissolved in NaCl/P_i; (3) fluorescein-5-maleimide (FM), dissolved in 20 mM Na_3PO_4, pH 12; (4) pyrene-*N*-maleimide (PM), dissolved in methanol. All labels were purchased from Molecular Probes Inc.

Labelling. Stock solutions of label (5–10 mM) were prepared immediately before labelling. Label stocks were diluted to ≈ 1 mM in 2 mL freshly prepared MBP–apoptin (5 mg·mL^{-1}) in NaCl/P_i/1 mM EDTA and incubated overnight in the dark at 4 °C. For IA and FM colabelling, equimolar amounts of label were used. Reactions were stopped by adding 10 mM 2-mercaptoethanol. Nonconjugated label was removed by passing the sample twice over a 5-mL PD-10 column (Pharmacia), equilibrated in NaCl/P_i/1 mM EDTA. Labelled MBP–apoptin was stored in the dark at 4 °C. Incorporation of label per MBP–apoptin monomer (mol/mol) was calculated using eqn (1), where A_c is the absorbance of label bound to protein at concentration c (in mg·mL^{-1}), M is the molecular mass of MBP–apoptin (55.8 kDa), and ε_{label} is the absorption coefficient of the label (cm·M^{-1}):

$$A_c/\varepsilon_{label} \times M/c \quad (1)$$

Fluorescence measurements

All fluorescence emission and excitation spectra were recorded on a Perkin–Elmer LS-50B at room temperature. All samples were passed through 0.22-μm (Ultrafree-MC; Millipore) filters before measurements. If necessary, the MBP moiety was saturated with 1 mM maltose (Fluka). Spectra were measured five times and averaged. For IA → FM FRET, the apparent distance between labels (R) was deduced from energy transfer efficiency (E) using eqns (2) and (3), where F_{DA} is fluorescence intensity of donor in the presence of acceptor, F_D is fluorescence of donor alone, and R_o is the Förster radius, i.e. R where $E = 50\%$.

$$E = 1 - (F_{DA}/F_D) \quad (2)$$

$$R = R_0{}^6\nu[(1/E) - 1] \quad (3)$$

IA and NBD fluorescence. MBP–apoptin-IA and MBP–apoptin-NBD were diluted to 1 μM [monomer] in assay buffer (20 mM Hepes, pH 7.4, 50 mM NaCl, 1 mM EDTA). Fluorimeter settings were: excitation wavelength = 338 (IA) or 481 (NBD); emission wavelength = 400–600 nm (IA) or 500–700 nm (NBD); slit width = 2.5 nm (IA) or 8 nm (NBD); scan speed = 200 nm·min^{-1}. For time course measurements, MBP–apoptin-IA and MBP–apoptin-NBD were incubated at 10 μM [monomer] at 37 °C (in the dark), and samples were taken after 1, 3, 6 and 24 h. To compensate for concentration changes due to protein precipitation, all spectra were normalized to the Trp fluorescence of the MBP moiety (excitation = 280 nm; emission peak = 355 nm; slit width = 2.5–4 nm; scan speed = 200 nm·min^{-1}). At 37 °C, the loss of protein amounted to ≈ 10% over 24 h. We verified, using dynamic light scattering, that the hydrodynamic radius (R_H) of labelled MBP–apoptin complexes was indistinguishable from that of unlabelled MBP–apoptin and did not change as a result of incubation at 37 °C. Dynamic light scattering analysis was performed as described previously [2].

PM fluorescence. MBP–apoptin-PM with a label incorporation of 0.15 or 0.6 PM per apoptin monomer (mol/mol) was diluted to 1.5 μM [monomer] in NaCl/P_i/1 mM EDTA. Settings were: excitation wavelength = 341 nm; emission wavelength = 360–520 nm; slit width = 2.5–4 nm; scan speed = 200 nm·min^{-1}. For time course measurements, MBP–apoptin-PM was diluted to 10 μM [monomer] and incubated at 37 °C in the dark. To compensate for concentration changes, all spectra were normalized to the 377 nm monomer peak. To determine the effect of denaturant on MBP–apoptin-PM excimer fluorescence, we diluted MBP–apoptin-PM with a label incorporation of 0.3 (mol/mol) in 0.1 M Bistris/7 M guanidinium chloride/1 mM EDTA or in NaCl/P_i/1 mM EDTA/0.5% CHAPS (Sigma). Because oxygen quenches PM excimer fluorescence more efficiently than monomer fluorescence, we evaluated the

effect of flushing the assay buffer with argon. In oxygen-free buffer, excimer fluorescence increased by no more than 5% compared with the monomer peak. We found that increasing the label incorporation to more than 0.6 (mol/mol) led to nonspecific binding of PM to MBP, as deduced from a large Trp → PM FRET effect (excitation = 280 nm; emission = 300–440 nm; slit width = 2.5 nm; scan speed = 120 nm·min^{-1}) (data not shown). We noticed that the PM emission spectrum underwent changes after ≈ 12 h at 37 °C that we attributed to chemical modification of the label, possibly oxidation.

bis-ANS titration

MBP–apoptin and H_6-MBP were dialysed extensively against 20 mM Hepes (pH 7.4)/10 mM NaCl/1 mM maltose/1 mM EDTA. Refolded apoptin-H_6 was dialysed against 20 mM potassium phosphate (pH 6.5)/400 mM NaCl/2 mM $MgCl_2$. A stock solution of 10 mM bis-ANS (dipotassium salt; Molecular Probes) was prepared in 10 mM Tris/HCl (pH 8.0)/1 mM EDTA/20% ethanol and stored at −20 °C. For each round of titrations, bis-ANS stock was diluted to 0.5–1 mM in dialysis buffer, which was used as assay buffer. We tested for buffer effects on the emission spectrum of bis-ANS by combining 0.5 μM BSA (Roche) with 2 μM bis-ANS in the respective assay buffers. Protein was diluted to 0.1–1 μM [monomer], and bis-ANS was added in a stepwise fashion (up to 10 μM). Conversely, bis-ANS was diluted to 25–100 nM and titrated with protein up to 10 μM [monomer]. Fluorimeter settings were: excitation wavelength = 400 nm; emission wavelength = 450–600 nm; slit width = 2.5 nm (for BSA/bis-ANS), 4 (if [monomer] = 1 μM) or 6 nm; scan speed = 300 nm·min^{-1}. In all cases, the increase in the bis-ANS fluorescence peak at 490 nm (F_{490}) stabilized within 2 min of mixing. Furthermore, we did not observe significant differences in bis-ANS binding characteristics between subsequent apoptin protein batches and between fresh protein and protein that had been stored for ≈ 6 months (at 4 °C) (data not shown). F_{490} values were adjusted for bis-ANS background fluorescence (F_o) and absorption by free dye, known as the 'inner filter effect', using PM and subsequently normalized, yielding $|F_{490}|$. A_{400} of 10 μM free bis-ANS is 0.1, and A_{490} is 0.001.

$$|F_{490}| = \{(F_{obs} - F_0) \times 10^{[(A400 + A490)/2]}\}/F_{490,max} \quad (4)$$

Curve fitting. Titration curves were fitted by nonlinear regression analysis using PRISM 3.00 (Graphpad Software Inc.). $|F_{490}|$ was plotted as a function of bis-ANS or protein monomer concentration and fitted with either a one-site or two-site saturation binding isotherm. The maximum F_{490} at a given bis-ANS concentration was deduced from the titration of 25 nM bis-ANS with MBP–apoptin. We verified that this maximum was linear with respect to the bis-ANS concentration (10–100 nM bis-ANS; data not shown).

Acrylamide quenching of MBP–apoptin/bis-ANS. (1) 1 μM MBP–apoptin monomer was combined with 50 nM bis-ANS (monomer/dye = 20); (2) 200 nM monomer was combined with 1 μM bis-ANS (dye/monomer = 5). In each case, the slit width was 10 nm. Acrylamide (Bio-Rad) was added from a 5.6 M (40% w/w) stock in a stepwise fashion up to 400 mM. After adjustment for dilution effects (yielding F_{adj}), the quenching curve was then fitted with the Stern–Volmer equation (eqn 5), where F_o is the fluorescence of the label in the absence of quencher, K_Q is the quenching constant, and A is a constant that compensates for quenching of the MBP-bound bis-ANS moiety. Here, the value for A was 0.08–0.11. To determine the level of maximum quenching, we fitted plots of F_{adj} vs. [acrylamide] to a two-phase exponential decay curve: the difference in fluorescence between F_o and the plateau corresponded to 100% quenching.

$$F_0/F_{adj} = (1 + A) + K_Q[\text{acrylamide}] \quad (5)$$

Subunit exchange

Exchange assay, monitored by IA → FM FRET. To remove the remaining traces of unincorporated label, MBP–apoptin-IA and MBP–apoptin-FM were dialysed extensively against NaCl/P_i/1 mM EDTA (CelluSep T1; 3.5-kDa cut-off; Membrane Filtration Products Inc., Seguin, TX, USA.). Subsequently, MBP–apoptin-IA was mixed with MBP–apoptin-FM at a 10 : 1 label ratio and a total protein concentration of 10 μM [monomer]. If not mentioned otherwise, the exchange assay was performed in NaCl/P_i/1 mM EDTA/0.5% CHAPS. The mixture was incubated at 30 °C (dark), and samples were taken after 1, 3, 6, 9 and 24 h. Settings were: excitation wavelength = 338 nm; emission wavelength = 400–600 nm; slit width = 2.5–5 nm; scan speed = 200 nm·min^{-1}. To compensate for protein precipitation, spectra were normalized to the isosbestic point at 504 nm for each round of experiments. FRET was expressed as the ratio between the IA emission (485 nm) and the FM emission (518 nm), denoted as F_{FM}/F_{IA}. The progression of the exchange reaction was visualized by plotting F_{FM}/F_{IA} as the percentage of maximum F_{FM}/F_{IA} per round of experiments. We verified that the Trp-normalized emission spectra of MBP–apoptin-IA and MBP–apoptin-FM alone were equally sensitive to quenching and precipitation at 30 °C in all buffers tested. To test the effect of different types of detergent, we replaced CHAPS with Triton X-100 (Roche) or *N*-octyl thioglucoside (Roche). Because the ability to exchange subunits declined as MBP–apoptin aged, we labelled protein directly after purification and used it for up to 4 weeks after labelling.

Exchange assay with MBP–apoptin-H6 and MBP–apoptin-FM. MBP–apoptin-H_6 and MBP–apoptin-FM were combined at a 10 : 1 ratio (w/w) and at 10 μM [monomer] in 20 mM Hepes (pH 7.4)/2.5 mM imidazole (Fluka)/300 mM NaCl/0.5% CHAPS. After 1–24 h incubation at 30 °C, samples (corresponding to 600 μg protein each) were cleaned on a 500-μL column of Ni^{2+}/nitrilotriacetate/agarose (Qiagen). Columns were washed with 30 mM imidazole and eluted with 300 mM imidazole. The eluted protein was diluted in NaCl/P_i/1 mM EDTA. Concentrations of total protein and MBP–apoptin-FM were determined from Trp and FM fluorescence, respectively. The FM fluorescence was adjusted for the effect of different

imidazole concentrations. In a control experiment, we determined that MBP–apoptin-FM (mixed 1 : 10 with unlabelled MBP–apoptin) had negligible affinity for Ni^{2+}/nitrilotriacetate/agarose.

Exchange assay with MBP–apoptin-PM. MBP–apoptin-PM with a label incorporation of 0.6 (mol/mol) was diluted to 1 : 10 in unlabelled MBP–apoptin at a total concentration of 10 μM [monomer], after which the mixture was incubated at 30 °C. Samples were taken after 1–24 h.

Subunit exchange in cell lysates

Cell lines used were $CD31^-$ (normal diploid fibroblasts), SW480 (human primary colon carcinoma-derived cell line), and NW18 (SV40-transformed tumourigenic fibroblasts). Cells were harvested at ≈80% confluency, washed with cold NaCl/P_i, and lysed in 50 mM Hepes, pH 7.4, containing 250 mM NaCl, 5 mM EDTA, 10 mM NaF, 25 mM α-glycerophosphate (Sigma), 5 mM GSH (Roche), 1% CHAPS, 0.2% Triton X-100, and protease inhibitor cocktail (2×; Roche). Lysates were centrifuged and then clarified using 0.22 μm filters. Directly before the exchange assay, $MgCl_2$ and ATP were added to 25 and 1 mM, respectively. A mixture of MBP–apoptin-IA and MBP–apoptin-FM was diluted to 5% (w/w) of total cellular protein (≈ 2 mg·mL^{-1}). Previous experiments indicated that MBP–apoptin is not significantly affected by proteolysis under these conditions.

Size distribution analysis of MBP–apoptin in cell lysates

Saos-2 and VH10 cells were grown to ≈50% confluency. Cells were washed with cold NaCl/P_i and harvested in ice-cold 25 mM Hepes, pH 7.4, containing 150 mM KCl, 2 mM $MgCl_2$, 5 mM dithiothreitol, 2.5 mM benzamidine/HCl (Sigma), 0.25% CHAPSO (Sigma). The suspensions were sonicated on ice, after which insoluble material was removed by centrifugation at 29 000 ***g*** for 20 min. After the respective protein concentrations had been determined, MBP–apoptin was added to 5% of total protein (w/w). As a control, MBP–apoptin was incubated in lysis buffer alone. Samples were incubated for 30 min at 30 °C, in the presence of 1 mM ATP and 20 mM $MgCl_2$, and 24 h at 4 °C, without additives. After incubation, samples were fractionated on a Superose 6 HR 10/30 analytical gel-filtration column (Amersham). Before fractionation, any precipitated material was pelleted by centrifugation at 29 000 ***g*** for 20 min, after which the pellets were washed with lysis buffer. All pellets and fractions were denatured in 1% SDS/1% 2-mercaptoethanol (5 min at 95 °C), then dot-blotted (10 μL each per dot) on poly(vinylidene difluoride) membrane (Bio-Rad) and detected with the monoclonal antibody to apoptin mAb 111.3 (epitope: residues 18–23) [4].

Results

MBP–apoptin and refolded apoptin-H_6 contain a similar collection of conformers

We used two different apoptin protein constructs: an N-terminal MBP–apoptin fusion protein, which is expressed as soluble multimers in *E. coli*, and hexahistidine-tagged apoptin, which can be refolded *in vitro* into soluble multimers [2]. To analyse potential conformational differences of the apoptin moieties in these constructs, we titrated both MBP–apoptin and refolded apoptin-H_6 with the fluorescent dye bis-ANS. The fluorescence of bis-ANS, measured at 490 nm (F_{490}), is enhanced severalfold in response to solvent shielding and has been widely used to characterize hydrophobic sites of proteins [5–8].

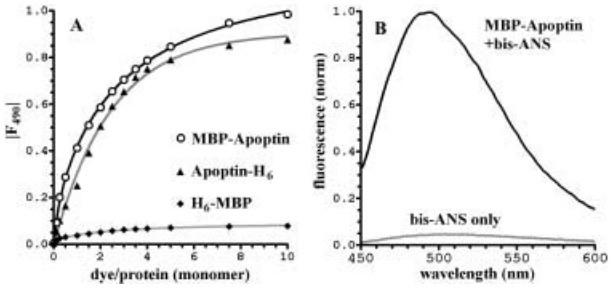

Fig. 1. Hydrophobic exposure of recombinant apoptin protein. (A) bis-ANS titration of refolded apoptin-H_6, MBP–apoptin and H_6-MBP. Protein concentration was 1 μM [monomer]. $|F_{490}|$ = increase in bis-ANS fluorescence, measured at 490 nm (normalized). (B) Emission spectrum of MBP–apoptin/bis-ANS, at a dye to monomer ratio of 5 : 1. In the presence of an excess of dye, the apoptin–bis-ANS complex had an emission maximum of 491 ± 1 nm, compared with 485 ± 1 nm when protein was in excess.

Binding of bis-ANS to MBP–apoptin and refolded apoptin-H_6 resulted in a ≈20-fold fluorescence increase (Fig. 1A,B), indicating that the apoptin multimer has a substantial hydrophobic surface. Compared with apoptin, MBP alone displayed little affinity for bis-ANS, provided that it was saturated with maltose. The emission spectrum of the apoptin–bis-ANS complex remained stable for at least 1 h at room temperature and for at least 24 h at 4 °C (data not shown), suggesting that multimeric apoptin does not contain any transiently exposed hydrophobic patches. Moreover, binding of bis-ANS to apoptin protein did not display co-operativity (Fig. 1A), indicating that dye binding itself did not induce the formation of hydrophobic pockets. Taking into account the contribution of the MBP moiety, the bis-ANS emission spectra and titration curves of MBP–apoptin and refolded apoptin-H_6 were very similar; control experiments with BSA indicated that the small difference in fluorescence yield could be explained by the different buffer conditions (data not shown). It is therefore likely that the two types of recombinant protein share a similar collection of conformers.

The majority of the monomers in the apoptin multimer belong to a single population

To probe the conformational uniformity of the apoptin subunits within the MBP–apoptin multimer, we quantified bis-ANS binding in titration experiments. We first determined the number of dye molecules bound per apoptin monomer. When we titrated bis-ANS with MBP–apoptin, we obtained a titration curve that was best fitted with a two-site binding isotherm (Fig. 2A). The apoptin–bis-ANS

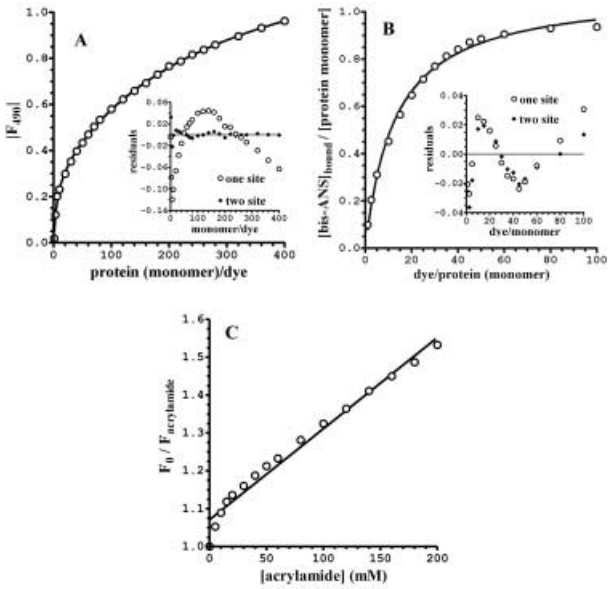

Fig. 2. The majority of the monomers in the apoptin multimer belong to a single population. (A) Titration of 25 nM bis-ANS with MBP–apoptin, fitted with a two-site binding isotherm. Inset: residuals of one-site and two-site binding isotherm fits. (B) Titration of 100 nM MBP–apoptin monomer, fitted with a two-site binding isotherm. Inset: residuals of one-site and two-site binding isotherm fits. (C) Stern–Volmer plot of acrylamide quenching of MBP–apoptin–bis-ANS. 1 μM [monomer] was mixed with 50 nM bis-ANS (monomer to dye ratio of 20 : 1). An acrylamide quenching experiment at a monomer to dye ratio of 1 : 5 produced essentially the same result. In this curve, quenching reached ≈ 90% of maximum.

complex apparently gave rise to two separate fluorescence maxima: one at a 20-fold molar ratio of protein monomer to dye ($F_{max} \cong 0.3$) and one at a ≈ 600-fold molar ratio ($F_{max} \rightarrow 1$). As the second F_{max} occurred at higher protein concentrations (≥ 10 μM [monomer]), we attributed this effect to clustering of apoptin multimers, although impurities in the MBP–apoptin preparation could also be a contributing factor. Multimer clustering possibly increases solvent shielding of bound dye, thereby enhancing its fluorescence yield. Because we did not detect any multimer clusters by gel filtration (up to 0.4 μM [monomer]) and dynamic light scattering analysis (0.4–10 μM [monomer]) [2], any such clusters are likely to be short-lived. Assuming that the first fluorescence maximum corresponded to an apoptin–bis-ANS complex without multimer interactions, we determined the concentration of bound and free dye in an MBP–apoptin/bis-ANS titration curve, and deduced that apoptin bound about one molecule of dye per monomer (Fig. 2B). As the fit of a one-site isotherm deviated only marginally from the two-site model (Fig. 2B), we concluded that most of the monomers within the apoptin multimer had a similar hydrophobic exposure.

Next, we evaluated the solvent exposure of apoptin–bis-ANS by acrylamide quenching. A plot of fluorescence quenching (F_Q/F_o) as a function of the concentration of the quenching agent [Q], termed a Stern–Volmer plot, reflects the number of different fluorophore populations [9,10]. The Stern–Volmer plot of MBP–apoptin–bis-ANS, shown in Fig. 2C, suggested that most if not all of the bound bis-ANS molecules experienced the same level of solvent exposure, with a K_Q of 2.4 ± 0.1 M^{-1}. A minor fraction of complexes had increased exposure, with a K_Q of 6.8 ± 0.8 M^{-1}. It is probable that the latter group of dye molecules corresponded to MBP-bound bis-ANS. Taken together, these results indicate that, despite the absence of regular secondary structure [2], the distribution of apoptin conformers is largely uniform.

The C-terminal domain of apoptin has an ordered and stable conformation

Under nondenaturing conditions, freshly prepared MBP–apoptin multimers reacted with the cysteine-specific dye Nbs_2 [3] at a stoichiometry of about 0.75 (mol/mol) Nbs_2 per MBP–apoptin monomer. A similar stoichiometry was observed with an MBP–apoptin mutant [MBP–apoptin(C30/47/49S) in which the three of the four Cys residues of MBP–apoptin were replaced with Ser]. This result indicated that the remaining Cys90, located in the C-terminal domain of the apoptin moiety, is the only reactive cysteine. The stoichiometry of 0.75 reflects the presence of C-terminally truncated monomers in the apoptin multimer [2].

To evaluate the geometric distribution of apoptin monomers within the multimeric complex, we labelled the reactive Cys90 of MBP–apoptin with PM. A well-documented feature of pyrene fluorescence is the formation of excimer pairs [11,12]. Pyrene excimer fluorescence is characterized by a broad emission peak at 465 nm and occurs when an excited-state pyrene interacts with a coplanar, ground-state pyrene less than 1 nm away. The pyrene monomer peak at 377 nm is essentially independent of excimer fluorescence and was therefore used to normalize spectra [11,12].

In comparison with the free PM−2-mercaptoethanol adduct, MBP–apoptin–PM, with a label incorporation of 0.15–0.6 (mol/mol), displayed a significant level of excimer fluorescence, indicating that at least some of the Cys90 sites of apoptin are in close proximity (Fig. 3A). We estimated that the PM labels were separated by 0.5–1 nm. Even in 7 M guanidinium chloride, the excimer fluorescence largely remained intact, indicating a substantial conformational stability of the C-terminal domain of MBP–apoptin to which the fluorescent label was attached (Fig. 3B). In addition, we failed to detect significant Trp → PM FRET in MBP–apoptin-PM, even though MBP contains eight Trp residues (data not shown) [13]. As the Förster radius for Trp → PM FRET is 2.8 nm [14] and as there are no Trp residues within the apoptin moiety, this finding indicated that the MBP moiety is not in direct contact with apoptin. Moreover, both moieties remained separated when MBP–apoptin-PM was incubated in $NaCl/P_i$ at 37 °C for up to 24 h.

We confirmed the stability of the C-terminal domain of apoptin by labelling MBP–apoptin with the environment-sensitive fluorescent probes IA and NBD. Both IA and NBD display enhanced fluorescence intensity in response to decreasing solvent exposure, which is accompanied by blue-shifting of their respective emission maxima [15,16]. The emission spectra of MBP–apoptin-IA and MBP–apoptin-NBD were symmetrical and had a half-maximal peak width comparable to that of the free 2-mercaptoethanol adduct

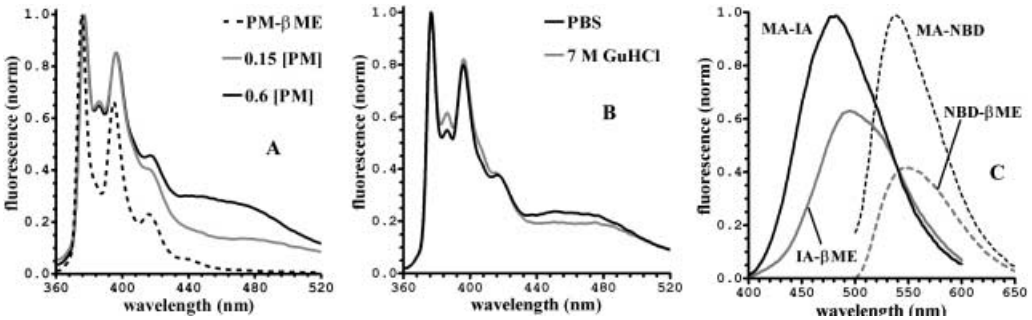

Fig. 3. The C-terminal domain of apoptin has an ordered and stable conformation. (A) Emission spectra of PM-2-mercaptoethanol and MBP–apoptin-PM with a label incorporation of 0.15 or 0.6 (mol/mol). (B) Effect of strong denaturant (7 M guanidium chloride) on pyrene excimer fluorescence in MBP–apoptin-PM [incorporation = 0.3 (mol/mol)]. (C) Emission spectra of MBP–apoptin (MA) labelled with IA and NBD. MBP–apoptin-IA had an emission maximum of 482 nm, compared with 492 nm for IA-2-mercaptoethanol, and its fluorescence intensity was increased by ≈ 40%. MBP–apoptin-NBD had a maximum of 538 nm, compared with 547 nm for NBD-2-mercaptoethanol, and its fluorescence intensity was increased approximately twofold. In theory, full solvent shielding would blue-shift IA fluorescence to ≈ 460 nm and increase the fluorescence intensity of NBD approximately fivefold [13,14].

(Fig. 3C), suggesting a uniform environment of Cys90 sites. We estimated that the labels of both MBP–apoptin-IA and MBP–apoptin-NBD were ≈ 50% solvent-exposed. Their fluorescence properties were not significantly affected when the labelled proteins were incubated in NaCl/P_i at 37 °C for up to 24 h (data not shown). Apparently, neither the IA nor the IA label experienced an increase or decrease in solvent exposure under these conditions. We therefore concluded that the C-terminal domain of apoptin did not undergo any significant structural rearrangements.

A minority of MBP–apoptin subunits are exchanged between multimers

To test for subunit exchange between apoptin multimers, we developed an assay based on the occurrence of FRET between IA and FM, both attached to apoptin Cys90. The IA label can act as a FRET donor for FM with a Förster radius of 4.6 nm [17]. Having established that the Cys90 sites of apoptin were in close proximity and had an apparently stable configuration, IA → FM FRET was likely to produce a strong effect that would not be affected by structural rearrangements. Exchange of subunits between MBP–apoptin labelled with IA and other multimers labelled with FM was expected to produce new FRET contacts. If so, we would be able to both identify and quantify subunit exchange from an increase in the ratio between FM and IA fluorescence (denoted as F_{FM}/F_{IA}), after excitation of IA.

The average label incorporation was 0.75 and 1.5 (mol/mol) per apoptin monomer for MBP–apoptin-FM and MBP–apoptin-IA, respectively. The occurrence of a strong Trp → IA FRET effect indicated that the 'excess' of IA label was attached to the MBP moiety, and not to a secondary site on apoptin (data not shown). The Förster radius for Trp → IA FRET is 2.2 nm [13], and the MBP and apoptin moieties are at least 2.8 nm apart, as mentioned above. Because of the strong distance dependence of FRET, and the long flexible linker between the apoptin and MBP moieties, the contribution of any MBP-bound IA to apoptin-IA → FM FRET is negligible.

To evaluate the efficiency of apoptin-IA → FM, we first colabelled MBP–apoptin with both IA and FM. Because IA contains a more reactive Cys-coupling group, we obtained MBP–apoptin-IA/FM with an IA to FM ratio of ≈ 10 : 1. Co-labelled MBP–apoptin-IA/FM displayed very efficient IA → FM FRET (Fig. 4A). Assuming that half of all incorporated IA labels were situated on the MBP moiety (≈ 75% of monomers contain Cys90 [2]), apoptin-IA → FM FRET was ≥ 95% efficient. Because the IA label is small and its fluorescence lifetime is relatively long (10–15 ns), we assumed that the influence of the orientation of IA with respect to FM averaged out [18]. Thus, we deduced that the FRET efficiency corresponded to an apoptin-IA to apoptin-FM distance of no more than 2.8 nm.

When MBP–apoptin-IA was combined with MBP–apoptin-FM in NaCl/P_i at a 10 : 1 molar ratio of incorporated label and incubated at 30 °C, we observed a clear increase in F_{FM}/F_{IA} over the course of 24 h (Fig. 4B). The increase reached a half-maximal effect after 2–3 h (Fig. 4D). This result was corroborated by incubating MBP–apoptin-PM with a 10-fold excess of unlabelled MBP–apoptin, which caused a fall in excimer fluorescence of ≈ 15%, presumably through dilution of PM-labelled monomers (Fig. 4C). As a control, we performed an exchange assay using MBP–apoptin-FM that had been fixed by covalently cross-linking it with glutaraldehyde [2]. We found that the increase in F_{FM}/F_{IA} with cross-linked MBP–apoptin-FM amounted to ≈ 15% of the effect we observed with noncross-linked protein, indicating that subunit exchange is the dominant factor in IA → FM FRET (Fig. 4D).

Supplementing the buffer with EDTA, Mg^{2+} or Zn^{2+} or varying the ionic strength between 0 and 300 mM NaCl had little effect on the rate and final extent of the exchange reaction. Moreover, subunit exchange in MBP–apoptin was largely independent of protein concentration, as tested at 2, 5 and 10 μM [monomer]. On addition of a fivefold molar excess of BSA, the rate of exchange was decreased by ≈ 10%, demonstrating that the interactions between multimers were only slightly shielded by the presence of an

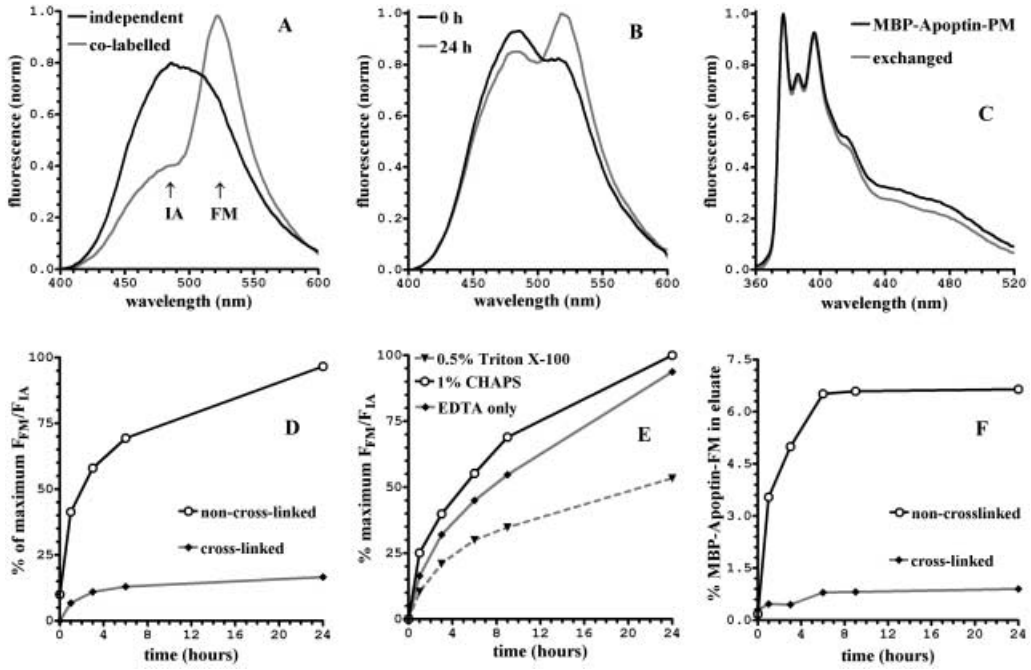

Fig. 4. Apoptin protein multimers exchange subunits. (A) MBP–apoptin, colabelled with IA and FM at a label ratio of 10 : 1. Independent = theoretical spectrum of MBP–apoptin, labelled separately with IA and FM and combined at the same label ratio. (B) IA → FM FRET-based exchange assay. MBP–apoptin-IA and MBP–apoptin-FM were combined at an IA to FM ratio of 10 : 1 and incubated at 30 °C for 24 h. (C) MBP–apoptin-PM, incubated in a 10-fold molar excess of unlabelled MBP–apoptin and incubated at 30 °C for 6 h. (D) Subunit exchange between MBP–apoptin-IA and cross-linked and noncross-linked MBP–apoptin-FM. MBP–apoptin-FM was cross-linked by treating it with glutaraldehyde. (E) Exchange in NaCl/P_i/1 mM EDTA, supplemented with 0.5% Triton X-100 or 1% CHAPS. (F) Copurification of MBP–apoptin-FM, cross-linked and noncross-linked, with MBP–apoptin-H_6 on Ni^{2+} nitrilotriacetate/agarose.

excess of bulk protein (data not shown). Also Triton X-100 slowed down the exchange, and *N*-octyl thioglucoside caused nearly complete precipitation of MBP–apoptin within 1 h at 30 °C (data not shown). Because MBP alone did not precipitate under the same conditions, it seems that *N*-octyl thioglucoside interacted selectively with the apoptin multimer to induce its precipitation. We found that adding CHAPS enhanced the rate of exchange by ≈ 20% (Fig. 4E), and MBP–apoptin hardly precipitated at all in NaCl/P_i/1 mM EDTA/0.5% CHAPS. We adopted these conditions as standard assay buffer for subunit exchange.

Subsequently, we verified that the rise in F_{FM}/F_{IA} was directly correlated with the exchange of material between multimers. To this aim, we incubated MBP–apoptin containing a C-terminal hexahistidine tag (MBP–apoptin-H_6) with FM-labelled MBP–apoptin in a 10 : 1 molar ratio. At various time points, aliquots were passed over Ni^{2+}/nitrilotriacetate/agarose, and fluorescence of the binding and nonbinding fractions was measured. We determined the amount of MBP–apoptin-FM incorporated into MBP–apoptin-H_6 by measuring the ratio of FM vs. Trp fluorescence in the eluted protein. We found that the histidine-tagged multimers became enriched with MBP–apoptin-FM (Fig. 4F). We noticed that the actual transfer of material between apoptin multimers occurred somewhat faster than the rise in F_{FM}/F_{IA} (compare Fig. 4D,F). The physical exchange reached its half-maximal effect within 1 h, compared with 2–3 h for the F_{FM}/F_{IA} effect. In addition, physical exchange reached equilibrium after 6 h, whereas the apoptin-IA → FM FRET effect continued to rise after 6 h (Fig. 4D,E). These observations suggested that internal rearrangements contributed to the efficiency of apoptin-IA → FM FRET, possibly through diffusion within the multimer.

As MBP–apoptin-H_6 was present in excess, we assumed that the fraction of MBP–apoptin-FM that had been transferred after 24 h corresponded to the maximum number of subunits that could be exchanged per multimer. We found that this fraction was equivalent to ≈ 15% of the monomers per FM-labelled multimer. This percentage was consistent with the observation that the absolute FRET effect caused by subunit exchange amounted to 10–15% of the FRET effect in co-labelled MBP–apoptin (Fig. 4A,B). It was also consistent with the fall in excimer fluorescence in MBP–apoptin-PM (Fig. 4C). Therefore, we concluded that the apoptin multimer exchanges *in vitro* ≈ 15% of its monomer content at maximum.

Subunit exchange may be affected by cellular binding partners

To test whether the cellular environment modulates subunit exchange between apoptin protein multimers, we repeated our FRET-based assay in human cell lysates derived from one normal ($CD31^-$) and two tumour cell lines (SW480 and NW18). First, we verified the persistence of the apoptin multimers in cell extract by incubating MBP–apoptin in Saos-2 (tumour) or VH10 (normal) cell lysate, or in lysis

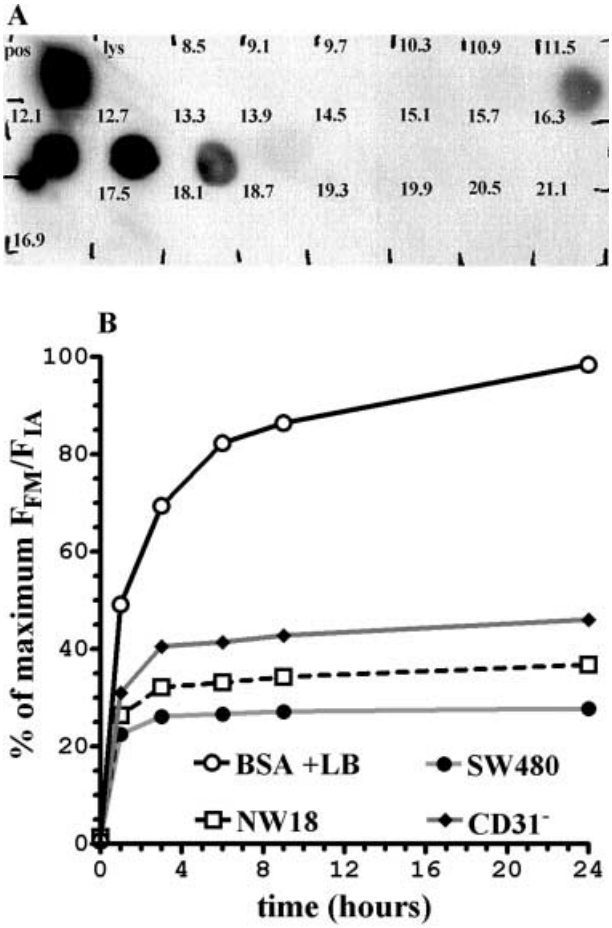

Fig. 5. Apoptin protein multimers do not dissociate in cell extract, but cellular factors may affect subunit exchange. (A) Dot-blot analysis of fractionation of MBP–apoptin on a Superose 6 HR 10/30 column, after incubation in Saos-2 cell lysate. pos = 50 ng MBP–apoptin; lys = lysate only. Fractions of 0.6 mL were collected, starting from the void volume at 8.5 mL. During calibration, the 670-kDa and 44-kDa markers were eluted at 13.8 and 17.2 mL, respectively. Blots were developed using apoptin antibody mAb 111.3. (B) Exchange in normal ($CD31^-$) and tumour (NW18 and SW480) cell lysate, compared with lysis buffer supplemented with BSA (BSA + LB).

buffer alone, as described in Materials and methods. Each sample was then fractionated on a Superose 6 HR 10/30 analytical gel filtration column, and analysed by dot-blot (Fig. 5A). We found that the size distribution of MBP–apoptin was not significantly altered in any of the samples [2], indicating that apoptin multimers do not dissociate in cell lysate.

The exchange experiments were performed in lysis buffer containing 0.1 $mg{\cdot}mL^{-1}$ MBP–apoptin; in activity assays, the intracellular concentration of MBP–apoptin after microinjection is 0.06–0.6 $mg{\cdot}mL^{-1}$ [19]. In the control experiment, BSA was added to the same concentration as cellular protein. We found that all cell lysates decreased the exchange rate 2 to 3-fold compared with the control (Fig. 5). We concluded that cellular factors influenced the exchange rate, perhaps by specifically binding to the surface of the apoptin multimer or by trapping exchangeable apoptin subunits. Judged from these results, a tumour-specific effect is at best tentative: the exchange rate in normal cell lysate ($CD31^-$) is marginally higher than in the fastest of the two normal cell lysates (NW18).

Discussion

Our finding that apoptin is active as a large multimer of 30–40 subunits prompted questions about the structure and dynamics of this complex and how these relate to its biological activity. Here, we present evidence that most of the apoptin moieties within the complex could well be sharing a similar conformation, irrespective of the recombinant construct examined. Titrations with bis-ANS indicated the presence of one hydrophobic binding site per apoptin monomer within the multimeric complex. Furthermore, these binding sites had uniform characteristics: the titration experiments suggested a single-site model. If apoptin had been present in a range of conformations, this could well have resulted in nonuniform binding of bis-ANS, requiring a multisite model. Also the fluorescence quenching experiments of apoptin-bound bis-ANS suggested a predominantly single-site model. Probing experiments with the covalently bound fluorophores PM, IA and NBD indicated considerable homogeneity and remarkable conformational stability of the apoptin monomers around the site of its attachment: residue Cys90. This is in agreement with our earlier finding that the OH of Tyr95 forms a stable hydrogen bond [2]. However, experiments monitoring subunit exchange between apoptin multimers indicated that $\approx 15\%$ of the subunits were exchangeable, whereas the bulk of the subunits did not exchange. The apparent disagreement of these observations, i.e. all subunits are equivalent vs. some subunits can exchange but others cannot, may be explained by the greater sensitivity of the exchange experiments. Indeed, careful analysis of both the bis-ANS titrations and the labelling experiments indicated that a small percentage of the apoptin monomers behaved differently from the bulk.

Exchange of subunits was significantly reduced in cell extracts, suggesting that cellular factors interact with the apoptin moieties. Although the reduction in exchange rate was more pronounced in tumour cell lysates, our current results cannot substantiate a significant tumour-specific or normal-specific effect. *In vivo* monitoring of subunit exchange by FRET may be required to settle this issue.

Our observations are consistent with a structural model in which apoptin forms a stable core of about 30–40 nonexchangeable subunits in which the monomers adopt a uniform and possibly unique conformation. However, we cannot exclude the possibility that several related, perhaps quasi-equivalent conformations, are trapped within the core of the apoptin multimer. In addition, we have to assume the presence of three to six additional, exchangeable monomers per multimer that bind less tightly. Earlier we showed that the N-terminal residues 1–69 of apoptin are sufficient for multimerization. These residues are largely hydrophobic, whereas the C-terminal part of apoptin is significantly more hydrophilic, containing many positively charged side chains. In view of the titration experiments with the hydrophobic dye bis-ANS, we have to assume that the nonexchangeable core structure of the apoptin complex has substantial

hydrophobic patches. It may well be that the hydrophobic N-termini of the exchangeable apoptin subunits interact nonspecifically with these patches. Our experiments indicating that detergents, but not ionic strength, influence the exchange reaction were in agreement with the hydrophobic nature of such interactions. The C-terminal part of apoptin does not form large multimers, but instead seems to dimerize or trimerize [2]. PM fluorescence suggested that the Cys90 residues within the multimeric complex are about 0.5–1 nm apart, and this distance may reflect the geometry of the proposed trimer.

Our results suggest aspects of apoptin structure that are important for triggering tumour-specific apoptosis. It is known that phosphorylation of Thr108 is required for this event [20], and it may be that the exchangeable apoptin subunits are more easily phosphorylated than the core apoptin moieties. However, in previous experiments, we demonstrated that extensively cross-linked apoptin is equally active in inducing cell death [2] and here we demonstrated that exchange of subunits no longer occurred in cross-linked apoptin. Therefore, it may well be that the exchangeable apoptin subunits are of less biological relevance and that their occurrence within the apoptin multimer is a mere consequence of nonspecific interactions with the hydrophobic patches on the multimer. Instead we propose that the multimer is the relevant biological structure. When phosphorylated, it may well provide a unique structural platform with extensive hydrophobic patches and stable, positively charged C-terminal domains, on which cellular factors within the nucleus organize to signal apoptosis.

References

1. Zhang, Y.-H., Leliveld, S.R., Kooistra, K., Molenaar, C., Rohn, J.L., Tanke, H.J., Abrahams, J.P. & Noteborn, M.H.M. (2003) Recombinant Apoptin multimers kill tumor cells but are non-toxic and epitope-shielded in a normal-cell-specific fashion. *Exp. Cell Res.* (in press).
2. Leliveld, S.R., Zhang, Y.-H., Rohn, J.L., Noteborn, M. & Abrahams, J.P. (2003) Apoptin induces tumor-specific apoptosis as a globular multimer. *J. Biol. Chem.* **278**, 9042–9051.
3. Riddles, P.W., Blakeley, R.L. & Zerner, B. (1983) Reassessment of Elmann's reagent. *Methods Enzymol.* **91**, 49–60.
4. Danen-van Oorschot, A.A., Fischer, D., Grimbergen, J., Klein, B., Zhuang, S.-M., Falkenburg, J., Backendorf, C., Quax, P., Van der Eb, A. & Noteborn, M. (1997) Apoptin induces apoptosis in human transformed and malignant cells but not in normal cells. *Proc. Natl. Acad. Sci. USA* **94**, 5843–5847.
5. Vanderheeren, G. & Hanssens, I. (1994) Thermal unfolding of bovine α-lactalbumin. *J. Biol. Chem.* **269**, 7090–7094.
6. Sharma, K., Kaur, H., Kumar, G. & Kester, K. (1998) Interaction of 1,1-bis(4-anilino)naphthalene-5,5′-disulfonic acid with α-crystallin. *J. Biol. Chem.* **273**, 8965–8970.
7. Bhattacharyya, A., Mandal, A., Banerjee, R. & Roy, S. (2000) Dynamics of compact denatured states of glutaminyl-tRNA synthetase probed by bis-ANS binding kinetics. *Biophys. Chem.* **87**, 201–212.
8. Smoot, A., Panda, M., Brazil, B., Buckle, A., Fersht, A. & Horowitz, P. (2001) The binding of bis-ANS to the isolated GroEL apical domain fragment induces the formation of a folding intermediate with increased hydrophobic surface not observed in tetradecameric GroEL. *Biochemistry* **49**, 4484–4492.
9. Deb, S., Bandyopadhyay, S. & Roy, S. (2000) DNA sequence dependent and independent conformational changes in multipartite operator recognition by l repressor. *Biochemistry* **39**, 3377–3383.
10. Fonseca, M., Scofano, H., Carvalho-Alves, P., Barrabin, H. & Mignaco, J. (2002) Conformational changes of the nucleotide site of the plasma membrane Ca^{2+}-ATPase probed by fluorescence quenching. *Biochemistry* **41**, 7483–7489.
11. Lehrer, S. (1997) Intramolecular pyrene excimer fluorescence: a probe of proximity and protein conformational change. *Methods Enzymol.* **278**, 286–295.
12. Panse, V., Vogel, P., Trommer, W. & Varadarajan, R. (2000) A thermodynamic coupling mechanism for the disaggregation of a model peptide substrate by chaperone SecB. *J. Biol. Chem.* **275**, 18698–18703.
13. Quiocho, F., Spurlino, J. & Rodseth, L. (1997) Extensive features of tight oligosaccharide binding revealed in high-resolution structures of the maltodextrin transport/chemosensory receptor. *Structure* **5**, 997–1015.
14. Wu, P. & Brand, L. (1994) Resonance energy transfer: methods and applications. *Anal. Biochem.* **218**, 1–13.
15. Spruijt, R., Wolfs, C., Verver, J. & Hemminga, M. (1996) Accessibility and environment probing using cysteine residues introduced along the putative transmembrane domain of the major coat protein of bacteriophage M13. *Biochemistry* **35**, 10383–10391.
16. Jensen, A., Guarnieri, F., Rasmussen, G., Asmar, F., Ballesteros, J. & Gether, U. (2001) Agonist-induced conformational changes at the cytoplasmic side of transmembrane segment 6 in the β2 adrenergic receptor mapped by site-selective fluorescent labelling. *J. Biol. Chem.* **276**, 9279–9290.
17. Nyitrai, M., Hild, G., Lakos, Z. & Somogyi, B. (1998) Effect of Ca^{2+}-Mg^{2+} exchange on the flexibility and/or conformation of the small domain in monomeric actin. *Biophys. J.* **74**, 2474–2481.
18. Andley, U. & Clark, B. (1988) Accessibilities of the sulfhydryl groups of native and photooxidized lens crystallins: a fluorescence lifetime and quenching study. *Biochemistry* **27**, 810–820.
19. Minascheck, G., Bereiter-Hahn, J. & Bertholdt, G. (1989) Quantitation of the Volume of liquid injected into cells by means of pressure. *Exp. Cell Res.* **183**, 434–442.
20. Rohn, J.L., Zhang, Y.-H., Aalbers, R., Otto, N., den Hertog, J., Henriquez, N., van de Velde, J., Kuppen, P., Mumberg, D., Donner, P. & Noteborn, M.H.M. (2002) A tumor-specific kinase activity regulates the viral death protein Apoptin. *J. Biol. Chem.* **277**, 50820–50827.